Chemical Science

ROYAL SOCIETY OF CHEMISTRY

EDGE ARTICLE

View Article Online
View Journal | View Issue

Check for updates

Cite this: *Chem. Sci.*, 2020, **11**, 12109

All publication charges for this article have been paid for by the Royal Society of Chemistry

Received 20th July 2020
Accepted 7th October 2020

DOI: 10.1039/d0sc03958f

rsc.li/chemical-science

Phenylene-bridged bis(benzimidazolium) ($BBIm^{2+}$): a dicationic organic photoredox catalyst†

Takuya Kodama, [a] Maiko Kubo,‡[a] Wataru Shinji,‡[a] Kei Ohkubo *[bc] and Mamoru Tobisu *[a]

A dicationic photoredox catalyst composed of phenylene-bridged bis(benzimidazolium) ($BBIm^{2+}$) was designed, synthesised and demonstrated to promote the photochemical decarboxylative hydroxylation and dimerisation of carboxylic acids. The catalytic activity of $BBIm^{2+}$ was higher than that for a monocation analogue, suggesting that the dicationic nature of $BBIm^{2+}$ plays a key role in these decarboxylative reactions. The rate constant for the decay of the triplet–triplet absorption of the excited $BBIm^{2+}$ increased with increasing concentration of the carboxylate anion with a saturated dependence, suggesting that photoinduced electron transfer occurs within the ion pair complex composed of the triplet excited state of $BBIm^{2+}$ and a carboxylate anion.

Introduction

Given the widespread availability of carboxylic acids from nature and commercial sources, the decarboxylative transformation of carboxylic acid derivatives represents an attractive synthetic organic method.[1] However, the direct decarboxylation of unactivated carboxylic acids remains a challenge, and the use of stoichiometric amounts of metal oxidants,[2] or pre-activation to acid chlorides or activated esters, such as Barton esters[3] and *N*-(acyloxy)phthalimides (NHPI esters),[4] are still required. Although organic electron acceptors such as acridinium,[5] iminium,[6] phthalimide,[7] and cyanoarene[8] have been reported to promote the decarboxylation of carboxylic acids under photoirradiation conditions, a stoichiometric amount of these acceptors is needed for the reaction to reach completion. The use of transition metal catalysts and photoredox catalysts for the catalytic decarboxylative transformation of carboxylic acids has extensively been studied (Scheme 1). In transition metal catalysed reactions, the metal carboxylates are generated *in situ* and then undergo decarboxylation to produce an aryl-metal species (Scheme 1a).[1a,c–e] However, the substrates are limited to the highly activated aromatic carboxylic acids bearing electron-withdrawing groups, such as nitro or fluorine group(s), at the *ortho* position, except for the Ni/PPh_3-catalysed decarboxylative olefination of alkyl carboxylic acids.[9] The other catalytic method involves the use of photoredox catalysis,[1b,e,10] in which the photoinduced single electron oxidation of an alkyl carboxylate anion with a photoexcited catalyst occurs, with the formation of an alkyl carboxyl radical (Scheme 1b). The alkyl carboxyl radical then spontaneously undergoes decarboxylation to produce an alkyl radical, which can participate in subsequent reactions. However, the application of this protocol to simple carboxylic acids is still difficult due to their highly positive oxidation potentials (*e.g.*, CH_3COO^-: $E_{1/2}(CH_3COO^-/CH_3COO^{\bullet})$ = +1.47 V *vs.* SCE),[11] when commonly used ruthenium polypyridyl complexes are employed as a photoredox catalyst (*e.g.*, $Ru(bpy)_3^{2+}$; bpy = 2,2′-bipyridyl: $E_{1/2}$ ($^*Ru^{II}/Ru^{I}$) = +0.77 V *vs.* SCE).[12] The use of iridium complexes containing pyridine-based ligands bearing electron-withdrawing groups has recently emerged as viable photocatalysts for promoting the oxidative decarboxylation of simple aliphatic carboxylic acids.[13,14] However, these transition-metal complexes are expensive and potentially toxic.[15] In the light of the above situation, the development of a simple and robust catalyst system that

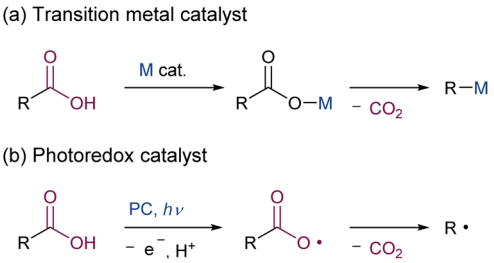

Scheme 1 Direct catalytic transformation of carboxylic acids.

[a]*Department of Applied Chemistry, Graduate School of Engineering, Osaka University, Suita, Osaka 565-0871, Japan. E-mail: tobisu@chem.eng.osaka-u.ac.jp*

[b]*Institute for Advanced Co-Creation Studies, Osaka University, Suita, Osaka 565-0871, Japan. E-mail: ohkubo@irdd.osaka-u.ac.jp*

[c]*Institute for Open and Transdisciplinary Research Initiatives, Osaka University, Suita, Osaka 565-0871, Japan*

† Electronic supplementary information (ESI) available. CCDC 1992124. For ESI and crystallographic data in CIF or other electronic format see DOI: 10.1039/d0sc03958f

‡ These authors contributed equally.

Open Access Article. Published on 07 October 2020. Downloaded on 8/28/2025 7:18:32 PM. This article is licensed under a Creative Commons Attribution-NonCommercial 3.0 Unported Licence.

Open Access Article. Published on 07 October 2020. Downloaded on 8/28/2025 7:18:32 PM.
This article is licensed under a Creative Commons Attribution-NonCommercial 3.0 Unported Licence.

enables oxidation of unactivated carboxylic acids without the use of harmful reagents would be highly desirable. Organic photoredox catalysts have the potential to address these issues.[16–18] An organic acridinium dye could be used in photocatalytic decarboxylative reactions of alkyl carboxylic acids including hydrodecarboxylation and decarboxylative trifluoromethylthiolation.[16,17] Yoshimi and co-workers reported on decarboxylative transformations of a wide variety of alkyl carboxylic acids using an arene/electron acceptor system by photoinduced electron transfer.[18,19] Although these examples demonstrate the potential utility of organic photoredox catalysts for use in oxidative decarboxylative transformation of unactivated organic acids, new classes of organic catalysts[20] continue to be developed to further expand the scope of these reactions.

We envisioned that dicationic organic salts could function as photoredox catalysts with high oxidation ability because their electron deficient nature allows the HOMO energy level to be lowered, thereby making the reduction potential in the excited state to be sufficiently high to allow carboxylates to be oxidised. To date, organic dicationic molecules have not been applied to photoredox reactions, except for 2,7-diazapyrenium,[21] trisaminocyclopropenium[22] and bisphosphonium.[23] Herein, we report on the design, synthesis and properties of a new dicationic organic photocatalyst based on a bis(benzimidazolium) ($BBIm^{2+}$) framework, and its application to photocatalytic decarboxylative reactions is also demonstrated.

Results and discussion

As cationic moieties, we focused on imidazolium scaffolds, which have found various applications in modern synthetic and material chemistry, for example, as precursors of *N*-heterocyclic carbenes[24] and components of ionic liquids.[25] Thermal stability,[26] redox properties,[27] and ease of structural modification would be desirable properties of such a catalyst. We designed a new phenylene-bridged bis(benzimidazolium) ($BBIm^{2+}$), with the expectation that two cationic imidazolium moieties should result in sufficiently low HOMO energies that would permit unactivated carboxylic acids to be oxidised upon photoexcitation (Scheme 2a). Density functional theory calculations at the ωB97XD/6-31G(d,p) level of theory were performed to investigate the structural and electronic properties of the $BBIm^{2+}$. Structural optimisation revealed that the benzimidazolium rings of $BBIm^{2+}$ are twisted relative to the central phenyl ring by 47° with a C_{2h} symmetry. The electrostatic potential indicated that the majority of the positive charges in $BBIm^{2+}$ are distributed over the imidazolium rings (Scheme 2c). $BBIm^{2+}$ possesses a lower HOMO ($\psi_{161} = -13.48$ eV) than that of monocation analogue $\mathbf{1}^+$ ($\psi_{91} = -11.60$ eV, Scheme 2d, *cf.* Fig. S5 in the ESI† for details), possibly because of the more positive nature of the molecule. These results indicate that $BBIm^{2+}$ would be reduced more easily than $\mathbf{1}^+$, thereby serving as a stronger oxidant than $\mathbf{1}^+$ as we initially envisioned. Indeed, the calculated HOMO energy of $BBIm^{2+}$ was lower than that of 9-mesityl-10-methylacridinium ($Acr\text{-}Mes^+$, $\psi_{83} = -11.24$ eV, *cf.* Fig. S5 in the ESI†), which can oxidize alkyl carboxylic acids in the photo excited state.[16,17] The HOMO of $BBIm^{2+}$ is distributed across the benzimidazolium and central phenylene rings, whereas the LUMO is largely located at the N=C–N moiety of the benzimidazolium ring and the phenylene moiety.

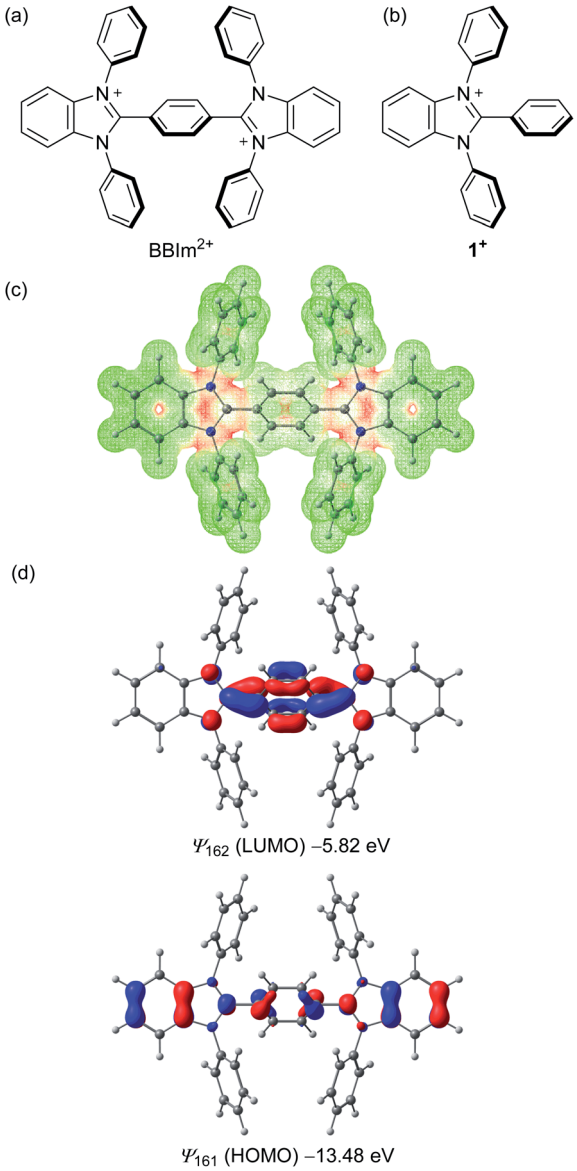

Scheme 2 Molecular structures of (a) $BBIm^{2+}$ and (b) monocation $\mathbf{1}^+$; (c) SCF potential (red positive and green negative) and (d) frontier orbitals (HOMO, LUMO) of $BBIm^{2+}$ generated by DFT calculations at the ωB97XD/6-31G(d,p) level of theory along with their energy levels.

Having estimated theoretically that $BBIm^{2+}$ has a sufficient oxidation ability to oxidise carboxylates by photoinduced electron transfer, we commenced our synthetic studies of $BBIm^{2+}$. $BBIm^{2+}$ was synthesised by a commonly used condensation reaction between a diamine and an aldehyde (Scheme 3).[28] Thus, the treatment of diamine **2** with terephthalaldehyde and a catalytic amount of *p*-toluenesulfonic acid afforded the double cyclised product **3** in 83% yield. Subsequent oxidation of **3** with *N*-bromoacetamide provided $BBIm^{2+}\cdot 2[Br^-]$. Because of the poor solubility of $BBIm^{2+}\cdot 2[Br^-]$ in common organic solvents,

This journal is © The Royal Society of Chemistry 2020

Open Access Article. Published on 07 October 2020. Downloaded on 8/28/2025 7:18:32 PM.
This article is licensed under a Creative Commons Attribution-NonCommercial 3.0 Unported Licence.

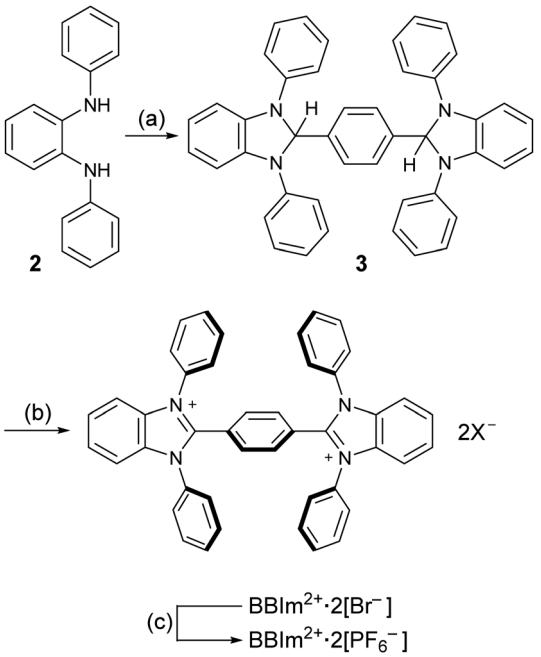

Scheme 3 Synthesis of $BBIm^{2+}\cdot 2[PF_6^-]$. [a]Reaction conditions: (a) terephthalaldehyde, *p*-TSA, $MgSO_4$, toluene, RT, 2 h, 83%. (b) *N*-Bromoacetamide, DMF, toluene, RT, 1 h. (c) $AgPF_6$, MeCN, RT, 1 h, 89% (2 steps). *p*-TSA = *p*-toluenesulfonic acid, DMF = *N*,*N*-dimethylformamide, RT = room temperature.

the counter anion was changed to PF_6^- by treatment with $AgPF_6$ in acetonitrile to give $BBIm^{2+}\cdot 2[PF_6^-]$ in 89% yield (2 steps from **3**), which is soluble in acetonitrile, DMF, and hexafluoroisopropanol.

Recrystallization from DMSO/methanol gave colorless crystals of $BBIm^{2+}\cdot 2[PF_6^-]$, which were suitable for a single X-ray crystallographic analysis (Fig. 1a, see Fig. S1 in ESI†). The dihedral angle for the central phenyl ring and benzimidazolium moieties was found to be 59° (Fig. 1b), which was larger than the calculated value. This difference can be attributed to the existence of counter anions and/or a packing force. The counter anions were located close to the imidazolium moieties in the crystal, in good agreement with the sites predicted based on the calculated electrostatic potential (Scheme 1b).

Absorption and emission spectra of $BBIm^{2+}\cdot 2[PF_6^-]$ (Fig. 2a) displayed an intense absorption band at around 290 nm with

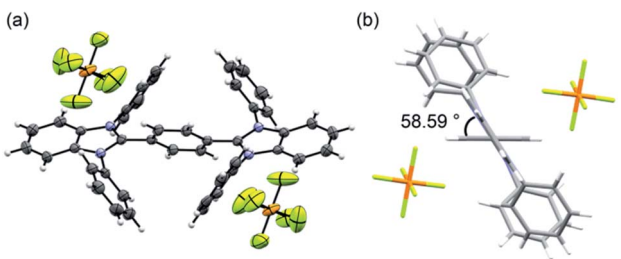

Fig. 1 (a) ORTEP drawing of $BBIm^{2+}\cdot 2[PF_6^-]$ at the 50% probability level and (b) side view of $BBIm^{2+}\cdot 2[PF_6^-]$.

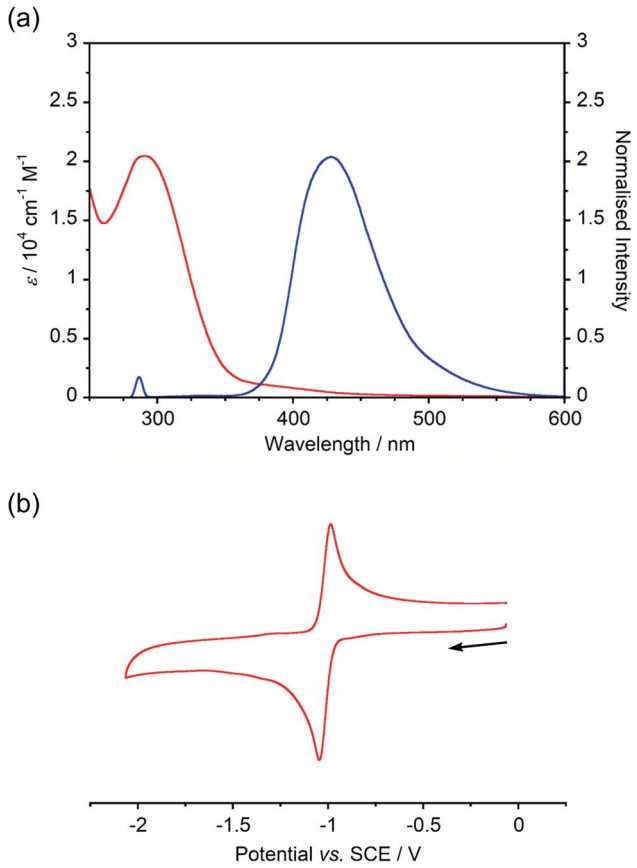

Fig. 2 (a) UV-vis absorption (red) and emission (blue) (λ_{ex} = 290 nm) spectra of $BBIm^{2+}\cdot 2[PF_6^-]$ (1.0×10^{-5} M in acetonitrile, room temperature); (b) cyclic voltammogram of $BBIm^{2+}\cdot 2[PF_6^-]$ (5.0×10^{-4} M in acetonitrile containing nBu$_4$NPF$_6$, room temperature, scan rate = 0.5 V s^{-1}).

a weak broad tail in the longer wavelength region (~500 nm), while a single emission peak with λ_{max} at 428 nm was observed. A large Stokes shift (~140 nm) of $BBIm^{2+}\cdot 2[PF_6^-]$ suggested that $BBIm^{2+}\cdot 2[PF_6^-]$ undergoes a significant structural change in the excited state. According to the time-dependent (TD) ωB97XD/6-31G(d,p) calculation of $BBIm^{2+}$, the absorption band at around 290 nm of $BBIm^{2+}$ is assigned to HOMO (ψ_{161}) → LUMO (ψ_{162}) transitions (λ = 288 nm and f = 0.99).

The cyclic voltammogram (CV) of $BBIm^{2+}\cdot 2[PF_6^-]$ in acetonitrile exhibited a reversible redox wave ($E_{1/2} = -1.02$ V *vs.* SCE) (Fig. 2b).[29] The corresponding monocation $\mathbf{1}^+\cdot[Br^-]$ displayed an irreversible wave ($E_{p/2} = -1.47$ V *vs.* SCE, Fig. S6 in ESI†). Therefore, the advantage of using $BBIm^{2+}\cdot 2[PF_6^-]$ over the corresponding monocation $\mathbf{1}^+\cdot[Br^-]$ can be attributed to not only its higher reduction potential as we initially envisioned, but also to the stability of the reduced species. Optical and electrochemical measurements led us to estimate the excited singlet state reduction potential of $BBIm^{2+}\cdot 2[PF_6^-]$ to be ${}^1E^*_{red} = +2.56$ V *vs.* SCE,[30] the value of which is sufficiently high to permit a wide variety of organic compounds such as benzene[31] or carboxylic acids to be oxidised.[11] The triplet state reduction potential of $BBIm^{2+}\cdot 2[PF_6^-]$ was also estimated to be ${}^3E^*_{red} = +0.89$ V *vs.* SCE.[30]

Open Access Article. Published on 07 October 2020. Downloaded on 8/28/2025 7:18:32 PM.
This article is licensed under a Creative Commons Attribution-NonCommercial 3.0 Unported Licence.

We next examined the catalytic activity of $BBIm^{2+}\cdot 2[PF_6^-]$ in the photocatalytic decarboxylative hydroxylation of carboxylic acids.[16] Irradiation of an acetonitrile solution of carboxylic acid **4a** with a xenon lamp (>300 nm) in the presence of $BBIm^{2+}\cdot 2[PF_6^-]$ (10 mol%) and NaOH (60 mol%) under an atmosphere of oxygen for 5 h afforded the desired alcohol **5a** in 68% yield, after reductive work up with $NaBH_4$ (Table 1, entry 1).[16b] Control experiments revealed that both $BBIm^{2+}\cdot 2[PF_6^-]$ and irradiation are essential for the reaction to efficiently proceed (entries 2 and 3). The reaction proceeded more efficiently under an atmosphere of oxygen compared with reactions performed under an atmosphere of nitrogen (entry 4). In the absence of NaOH, the yield was decreased to 32% (entry 5). The use of the corresponding monocation $\mathbf{1}^+\cdot[Br^-]$ (entry 6) or Acr-$Mes^+\cdot[ClO_4^-]$[16a,32] (entry 7) as a photocatalyst also gave **5a**, but in lower yields of 40% and 46%, respectively. In addition, the quantum yield for the photocatalytic hydroxylation reaction using $BBIm^{2+}\cdot 2[PF_6^-]$ was determined to be 0.60, which is significantly higher than that for $\mathbf{1}^+\cdot[Br^-]$ (0.004) or Acr-$Mes^+\cdot[ClO_4^-]$ (0.23) catalysed reactions.[33] The reaction also proceeded by using 365 nm or 405 nm LED lights instead of a xenon lamp (entries 8 and 9). It was possible to oxidise an array of carboxylic acids using $BBIm^{2+}$ under the optimised conditions (Table 2). Benzylic carboxylic acids bearing methyl (**4a**), phenyl (**4b**) and cyclohexyl (**4c**) groups at the benzylic position were successfully decarboxylated to give the corresponding benzyl alcohols (**5a–5c**) in good yields. Whereas primary benzylic (**4d**) and secondary non-benzylic (**4e**) carboxylic acids were not good substrates in this decarboxylative hydroxylation, tertiary alkyl carboxylic acids **4f** and **4g** underwent the reaction to give products in moderate to good yield.

Table 1 Photoinduced $BBIm^{2+}$-catalysed decarboxylative hydroxylation of **4a**[a]

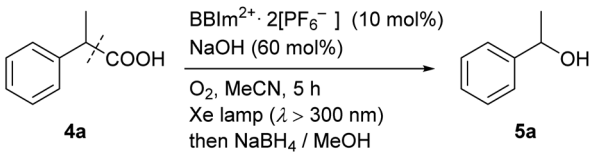

4a **5a**

Entry	Variation from the standard conditions	GC yields (%)
1	None	68
2	Without $BBIm^{2+}\cdot 2[PF_6^-]$	0
3	In the absence of light source	0
4	Under N_2	8
5	Without base	32
6	$\mathbf{1}^+\cdot[Br^-]$ instead of $BBIm^{2+}\cdot 2[PF_6^-]$	40
7	Acr-$Mes^+\cdot[ClO_4^-]$ instead of $BBIm^{2+}\cdot 2[PF_6^-]$	46
8	365 nm LED lamp (60 W) instead of Xe lamp	67
9	405 nm LED lamp (60 W) instead of Xe lamp	35

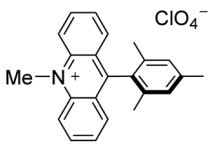

Acr-$Mes^+\cdot[ClO_4^-]$

[a] Reaction conditions: (a) **4a** (0.15 mmol), $BBIm^{2+}\cdot 2[PF_6^-]$ (0.015 mmol), NaOH (0.090 mmol), O_2, in acetonitrile (6.0 mL), xenon lamp (500 W) irradiation for 5 h, RT; (b) $NaBH_4$, MeOH.

Table 2 Substrate scope for $BBIm^{2+}$-catalysed decarboxylative hydroxylation[a]

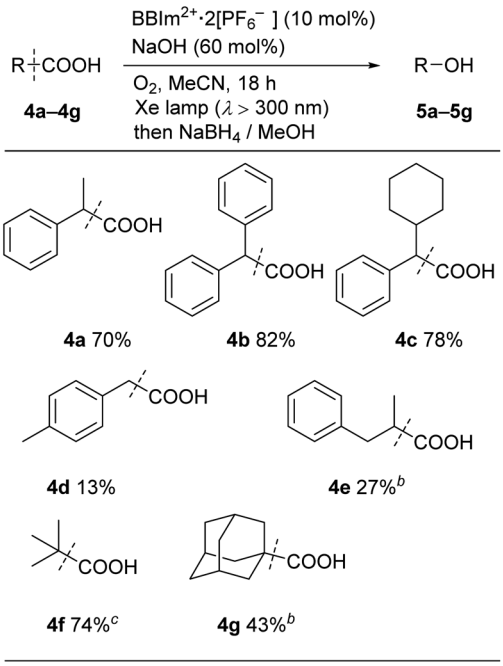

[a] Reaction conditions: carboxylic acid (0.15 mmol), $BBIm^{2+}\cdot 2[PF_6^-]$ (0.015 mmol), NaOH (0.090 mmol) in acetonitrile (6.0 mL), xenon lamp (500 W) irradiation for 18 h, RT. [b] GC yield. [c] NMR yield.

During the course of our investigation of photocatalytic decarboxylative hydroxylation reactions using $BBIm^{2+}\cdot 2[PF_6^-]$, we found that the tertiary benzylic carboxylic acid **6a** underwent decarboxylative dimerisation to give **7a** under identical conditions. Although this type of decarboxylative dimerisation reaction has already been reported, including Kolbe electrolysis[34a] and reactions using a stoichiometric amount of an oxidant, such as $S_2O_8^-$,[34b] and Hg(II),[34c] and a heterogeneous a Pt–TiO_2 photocatalyst,[14b,c] this is the first example of the use of an organic photoredox catalyst, to the best of our knowledge. Further optimization for this dimerisation was performed using **6a** as a substrate (Table 3). The yield of **7a** was increased when the reaction was carried out under an atmosphere of air rather than oxygen (entries 1 and 2). Finally, shortening the reaction time to 3 h resulted in a better yield, because the undesired decomposition of **7a** could be suppressed (57%, entry 3).[35] The use of the monocation $\mathbf{1}^+\cdot[Br^-]$ or Acr-$Mes^+\cdot[ClO_4^-]$[16a,32] as a catalyst resulted in lower yields of 4% and 33%, respectively (entries 4 and 5). These results again underscore the prominent activity of this dicationic catalyst for the oxidation of unactivated organic acids.

A range of tertiary benzylic carboxylic acids (**6a–6h**) could be oxidatively dimerised by $BBIm^{2+}\cdot 2[PF_6^-]$ under

 This journal is © The Royal Society of Chemistry 2020

Open Access Article. Published on 07 October 2020. Downloaded on 8/28/2025 7:18:32 PM.
This article is licensed under a Creative Commons Attribution-NonCommercial 3.0 Unported Licence.

Table 3 Photocatalytic decarboxylative dimerisation of **6a**[a]

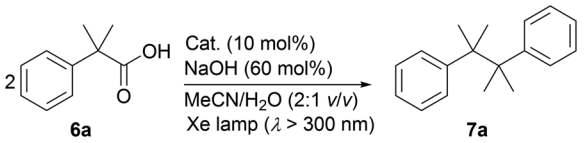

6a **7a**

Entry	Cat.	Atmosphere	Time (h)	NMR yields (%) 7a	6a
1[b]	$BBIm^{2+}\cdot 2[PF_6^-]$	O_2	18	23	0
2[b]	$BBIm^{2+}\cdot 2[PF_6^-]$	Air	18	47	1
3	$BBIm^{2+}\cdot 2[PF_6^-]$	Air	3	57	9
4	$\mathbf{1}^{+}\cdot[Br^-]$	Air	3	4	0
5	$Acr\text{-}Mes^{+}\cdot[ClO_4^-]$	Air	3	33	0

[a] Reaction conditions: **6a** (0.15 mmol), cat. (0.015 mmol), NaOH (0.090 mmol), in acetonitrile/H_2O (6.0 mL), xenon lamp (500 W) irradiation, RT. [b] The reaction was conducted in CH_3CN/H_2O (1 : 1).

photoirradiation to be converted to the corresponding dimers (Table 4). Benzylic carboxylic acids bearing a fluoro group on the phenyl ring, such as **6b** and **6c**, effectively underwent dimerisation. The introduction of a trifluoromethyl group, as in **6d**, decreased the yield of the dimerised product. Phenylacetic acids bearing a spiro ring system at the benzylic position, such as **6e** and **6f**, gave the corresponding dimers **7e** and **7f**. π-Extended derivatives, as represented by **6g** and **6h**, also served as good substrates for decarboxylative dimerisation. Aliphatic and secondary benzylic carboxylic acids failed to give any decarboxylative dimerisation products under these conditions, but alcohols, as in Table 2, were formed as products instead.

Table 4 Scope for photocatalytic decarboxylative dimerisation of tertiary-alkyl carboxylic acids[a]

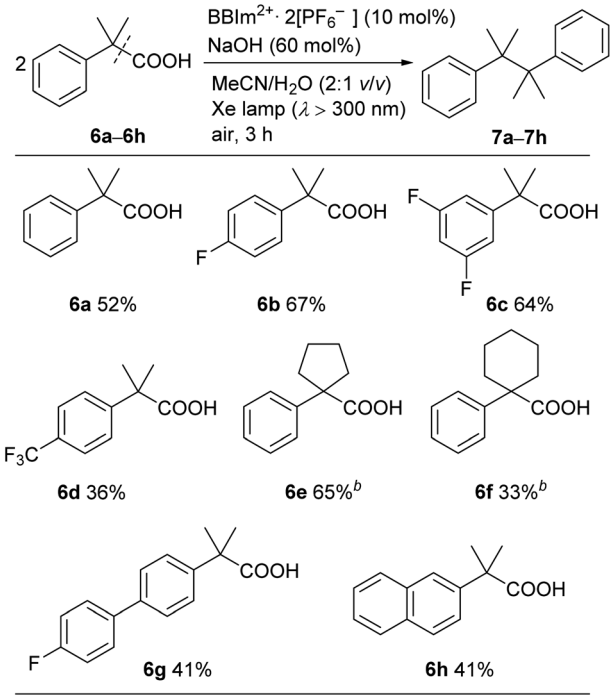

[a] Reaction conditions: carboxylic acid (0.15 mmol), $BBIm^{2+}\cdot 2[PF_6^-]$ (0.015 mmol), NaOH (0.090 mmol) in acetonitrile (4.0 mL)/H_2O (2.0 mL), xenon lamp (500 W) irradiation for 3 h, RT. [b] Run for 18 h.

To elucidate the mechanism for this photoinduced decarboxylation reaction, quenching measurements[36] were performed by fluorescence and triplet–triplet (T–T) absorption spectroscopies. Electron transfer from *t*BuCOO$^-$ to the singlet excited state of $BBIm^{2+}$ ($^1BBIm^{2+*}$) is energetically favorable because the free energy change is significantly negative: $\Delta G_{et} = E_{ox} - E_{red} - {}^1E^* = 1.02 - (-0.50) - 3.58 = -2.06$ eV. However, no fluorescence quenching was observed when *t*BuCOO$^-$ was added to an acetonitrile solution containing $BBIm^{2+}$. The fluorescence lifetime of $BBIm^{2+}$ was determined to be 0.4 ns by time-resolved fluorescence measurements, which is too short to quench the low concentration of *t*BuCOO$^-$ (0–0.2 mM) under the present experimental conditions.[37] It therefore appears that the reactive species may be the triplet excited state of $BBIm^{2+}$ ($^3BBIm^{2+*}$) rather than the short-lived singlet excited state. The free energy change for the electron transfer from *t*BuCOO$^-$ to $^3BBIm^{2+*}$ was estimated to be $\Delta G_{et} = E_{ox} - E_{red} - {}^3E^* = 1.02 - (-0.50) - 1.91 = -0.39$ eV, where $^3E^*$ was determined from the phosphorescence spectrum (λ_{max} = 641 nm) observed in an ethanol glass at 77 K. The negative ΔG_{et} value indicates that the electron transfer from *t*BuCOO$^-$ to $^3BBIm^{2+*}$ is energetically feasible. To observe the electron transfer process between *t*BuCOO$^-$ and $^3BBIm^{2+*}$, the T–T absorption measurements were carried out by nanosecond laser flash spectroscopy (Fig. 3a). A typical T–T absorption at $\lambda_{max} = 580$ nm was detected taken at 0.8 ms after laser excitation at 355 nm due to the absorption of $BBIm^{2+}$. The T–T absorption decays obeying first-order kinetics with the rate constant (k_T) of 1.9×10^2 s^{-1}. *t*BuCOO$^-$ was added to an acetonitrile solution of $BBIm^{2+}\cdot 2[PF_6^-]$ and the decay time profile was monitored at 580 nm. The observed decay rate constant (k_{obs}) increased with increasing concentration of *t*BuCOO$^-$, as shown in Fig. 3b. Interestingly, a saturated dependence was observed, rather than the typical linear relationship observed for a simple quenching

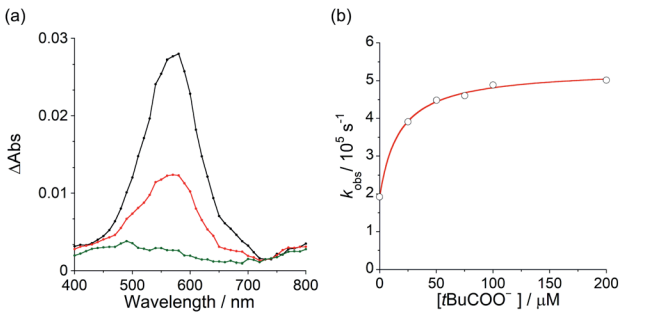

Fig. 3 (a) Transient absorption spectra of $BBIm^{2+}$ taken at 0.8 ms (black), 5 ms (red), 20 ms (green) after laser excitation at 355 nm in deaerated MeCN. (b) Dependence of decay rate constant of triplet–triplet absorption of $^3BBIm^{2+*}$ on the concentration of pivalate.

Open Access Article. Published on 07 October 2020. Downloaded on 8/28/2025 7:18:32 PM.
This article is licensed under a Creative Commons Attribution-NonCommercial 3.0 Unported Licence.

mechanism. The saturated behavior revealed that photoinduced electron transfer occurred with the formation of an ion pair complex composed of the $^3BBIm^{2+*}$ and tBuCOO$^-$, in competition with bimolecular electron transfer from tBuCOO$^-$ to $^3BBIm^{2+*}$ and triplet decay of $^3BBIm^{2+*}$ to the ground state without electron transfer (Scheme 4).[38] The association constant (K_{assoc}) for the formation of an encounter complex $^3BBIm^{2+*}\cdot[t\text{BuCOO}^-][PF_6^-]$ and the rate constant (k_{ET}) for intra-complex photoinduced electron transfer from tBuCOO$^-$ to $^3BBIm^{2+*}$ were estimated to be 5.8×10^5 M^{-1} and 3.4×10^2 s^{-1}, respectively, by curve fitting using eqn (1).

$$k_{obs} - k_T = k_{ET}K_{assoc}[t\text{BuCOO}^-]/[1 + K_{assoc}[t\text{BuCOO}^-]] \quad (1)$$

The electrochemical and optical properties of $BBIm^{2+}\cdot 2[PF_6^-]$ are summarised in Table 5 and an energy diagram of $BBIm^{2+}$ is shown in Scheme 4. The photoirradiation initially generates $^1BBIm^{2+*}$, which is not quenched with tBuCOO$^-$ by electron transfer under the experimental conditions. Intersystem crossing, which is in competition with the fluorescence decay bound for the ground state, results in the formation of $^3BBIm^{2+*}$. An intimate encounter complex between $^3BBIm^{2+*}$ and the anionic tBuCOO$^-$ substrate is formed, and electron transfer in the complex then occurs to produce a radical pair ($BBIm^{\bullet+}$/tBuCOO$^\bullet$). Based on the saturated behavior shown in Scheme 3b, an outer sphere electron transfer process from tBuCOO$^-$ to $^3BBIm^{2+*}$ is presumably significantly slower than the intra-complex electron transfer. No back electron transfer from $BBIm^{\bullet+}$ to tBuCOO$^\bullet$ occurs due to the rapid spontaneous decarboxylation of tBuCOO$^\bullet$ leading to the products.

A plausible reaction mechanism for decarboxylative hydroxylation and dimerisation is shown in Scheme 5. Photoredox catalyst $BBIm^{2+}$ is initially excited by photoirradiation and subsequent intersystem crossing generates $^3BBIm^{2+*}$, which oxidises the carboxylate **A** *via* single electron transfer (SET) to give

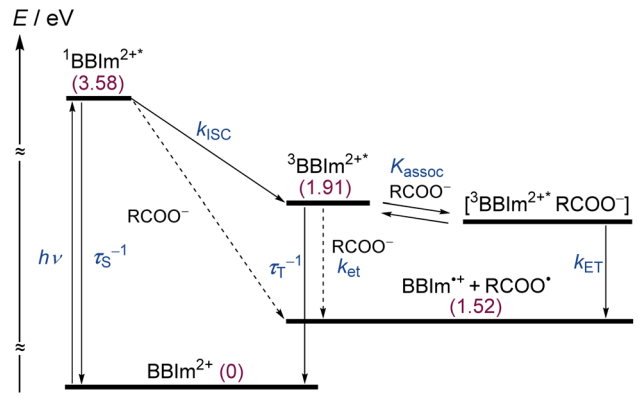

Scheme 4 Energy diagram of $BBIm^{2+}$. R = tBu, τ_S = fluorescence lifetime, τ_T = phosphorescence lifetime, k_{ISC} = rate constant for intersystem crossing, k_{et} = rate constant for electron transfer from tBuCOO$^-$ to $^3BBIm^{2+*}$, K_{assoc} = association constant for the formation of an encounter complex $^3BBIm^{2+*}\cdot[t\text{BuCOO}^-][PF_6^-]$, k_{ET} = rate constant for intra-complex photoinduced electron transfer from tBuCOO$^-$ to $^3BBIm^{2+*}$. Numbers in parentheses refer to energy levels of the species relative to $BBIm^{2+}$ in the ground state.

Table 5 Summary of the electrochemical and optical properties of $BBIm^{2+}\cdot 2[PF_6^-]$[a]

E_{red}/V	$^1E^*$/eV	$^1E^*_{red}$/V	$^3E^*$/eV	$^3E^*_{red}$/V	λ_{max}/nm	λ_{em}/nm	τ_S/ns
−1.02	+3.58	+2.56	+1.91	+0.86	290	428	0.4

[a] All potentials in V *vs.* SCE. E_{red} = ground state reduction potential, $^1E^*$ = singlet excitation energy, $^1E^*_{red}$ = excited singlet state reduction potential, $^3E^*$ = triplet excitation energy, $^3E^*_{red}$ = excited triplet state reduction potential. λ_{max} = absorption peak, λ_{em} = emission peak excited at 290 nm. τ_S = fluorescence lifetime.

the carboxyl radical B and the radical cation $BBIm^{\bullet+}$. The carboxyl radical **B** rapidly releases CO_2 to produce the alkyl radical **C**. Under an O_2 atmosphere, the generated radical **C** is captured by oxygen[39] to generate peroxyl radical **D** [E_{red} ($t\text{BuO}_2^\bullet/t\text{BuO}_2^-$) = +0.50 V *vs.* SCE],[16a,38] which is subsequently reduced by the radical cation $BBIm^{\bullet+}$ (E_{red} = −1.02 V *vs.* SCE) to form the peroxyl anion **E** with the regeneration of $BBIm^{2+}$. Anion **E** is prone to undergo disproportionation to generate a mixture of an alcohol and a ketone, which was isolated as a single alcohol product by treatment with $NaBH_4$ in this study. When the reaction is performed under an atmosphere of air, in which the oxygen concentration is relatively low, two alkyl radicals **C** undergo radical–radical coupling to form dimer **G** before it is captured by oxygen.[40] In this case, SET from the radical cation $BBIm^{\bullet+}$ to oxygen [$E_{red}(O_2/O_2^{\bullet-})$ = −0.86 V *vs.* SCE][41] regenerates the catalyst $BBIm^{2+}$ with the concomitant formation of superoxide ($O_2^{\bullet-}$), which is eventually reduced to hydrogen peroxide.[33]

The key to the successful application of $BBIm^{2+}$ in photocatalytic decarboxylative transformation of benzylic carboxylic acids is its dicationic nature, which serves to reduce the activation barrier of the SET from carboxylate by lowering the reorganization energy of the polar solvents.[31b,c] When an electronically neutral photocatalyst (PC) oxidises a monoanionic substrate (S^-), a radical anion of PC ($PC^{\bullet-}$) and a neutral radical ($S^\bullet$) are generated (Scheme 6a). In this process, the charges of the both components changes (PC: neutral → negative; S: negative → neutral), which requires the solvent molecules around PC and S

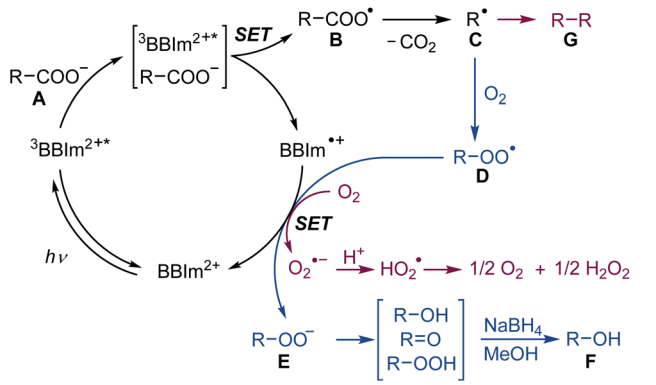

Scheme 5 Proposed mechanism for the photocatalytic hydroxylation under O_2 (blue) and dimerisation of carboxylic acids under an atmosphere of air (red). SET: single electron transfer.

This journal is © The Royal Society of Chemistry 2020

Open Access Article. Published on 07 October 2020. Downloaded on 8/28/2025 7:18:32 PM.
This article is licensed under a Creative Commons Attribution-NonCommercial 3.0 Unported Licence.

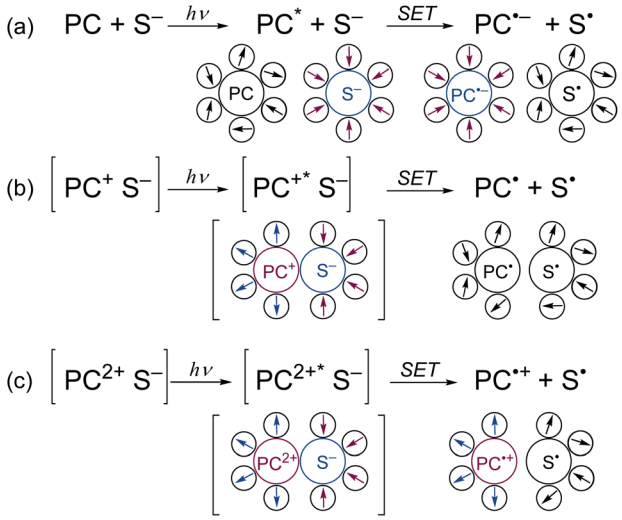

Scheme 6 Comparison of the reorganization of polar solvents during single electron transfer processes from monoanionic substrate (S^-) to (a) neutral, (b) monocationic, and (c) dicationic photocatalysts (PCs). Arrows represent the dipole moments of the solvents.

to be reorganised to form polarity-matched clusters. Similarly, a large solvent reorganization energy would be expected to be required when a monocationic PC is used (Scheme 6b, PC: positive → neutral; S: negative → neutral). In contrast, the reorganization energy becomes lower when a dicationic PC is used, since the sign of the charge of PC remains unchanged (Scheme 6c).[31c]

Conclusions

In conclusion, we report on the development of a novel dicationic photoredox catalyst $BBIm^{2+}$, the photophysical and electrochemical properties of which indicate that it has a strong oxidation ability in the excited state. In fact, $BBIm^{2+}$ was demonstrated to be a viable organic photocatalyst for promoting the decarboxylative hydroxylation and dimerisation of unactivated carboxylic acids. The striking feature of $BBIm^{2+}$ is its dicationic nature, which allows it to form an intimate ion pair with an anionic substrate, resulting in an energetically favorable SET process. Further development of new cationic organic photocatalysts and their application to otherwise difficult oxidative transformations is now ongoing in our laboratory.

Conflicts of interest

There are no conflicts to declare.

Acknowledgements

This work was supported by Scientific Research on Innovative Area "Hybrid Catalysis" (20H04818, 20H04819) and Grant-in-Aid for Early-Career Scientists (19K15564) from MEXT, Japan. MT wishes to thank the Hoansha Foundation for their financial support. We also thank Prof. Ikeda (Osaka Prefecture University) and Prof. Asahara (Osaka University) for helpful discussion and Prof. Minakata, Prof. Takeda, Prof. Kida, and Prof. Mori (Osaka University) for their assistance with the fluorescence lifetime measurements.

Notes and references

1 Selected reviews: (*a*) N. Rodríguez and L. J. Goossen, *Chem. Soc. Rev.*, 2011, **40**, 5030–5048; (*b*) J. Xuan, Z.-G. Zhang and W.-J. Xiao, *Angew. Chem., Int. Ed.*, 2015, **54**, 15632–15641; (*c*) H. Huang, K. Jia and Y. Chen, *ACS Catal.*, 2016, **6**, 4983–4988; (*d*) Y. Wei, P. Hu, M. Zhang and W. Su, *Chem. Rev.*, 2017, **117**, 8864–8907; (*e*) J. Schwarz and B. König, *Green Chem.*, 2018, **20**, 323–361.

2 (*a*) F. Minisci, R. Bernardi, F. Bertini, R. Galli and M. Perchinummo, *Tetrahedron*, 1971, **27**, 3575–3579; (*b*) Y. N. Ogibin, L. K. Rakhmatullina and G. I. Nikishin, *Russ. Chem. Bull.*, 1975, **24**, 2608–2613; (*c*) F. Minisci, E. Vismara and F. Fontana, *Heterocycles*, 1989, **28**, 489–519; (*d*) M. A. J. Duncton, *MedChemComm*, 2011, **2**, 1135–1161; (*e*) J. Kan, S. Huang, J. Lin, M. Zhang and W. Su, *Angew. Chem., Int. Ed.*, 2015, **54**, 2199–2203; (*f*) R. Xia, M.-S. Xie, H.-Y. Niu, G.-R. Qu and H.-M. Guo, *Org. Lett.*, 2014, **16**, 444–447.

3 (*a*) D. H. R. Barton, B. Lacher and S. Z. Zard, *Tetrahedron*, 1987, **43**, 4321–4328; (*b*) D. Crich and L. Quintero, *Chem. Rev.*, 1989, **89**, 1413–1432; (*c*) D. H. R. Barton and M. Ramesh, *Tetrahedron Lett.*, 1990, **31**, 949–952; (*d*) M. F. Saraiva, M. R. C. Couri, M. L. Hyaric and M. V. Almeida, *Tetrahedron*, 2009, **65**, 3563–3572; (*e*) X. Xu, P. Li, Y. Huang, C. Tong, Y. Yan and Y. Xie, *Tetrahedron Lett.*, 2017, **58**, 1742–1746.

4 (*a*) M. Dinda, C. Bose, T. Ghosh and S. Maity, *RSC Adv.*, 2015, **5**, 44928–44932; (*b*) I. B. Krylov, V. A. Vil' and A. O. Terent'ev, *Beilstein J. Org. Chem.*, 2015, **11**, 92–146; (*c*) Z. Guo, X. Jiang, C. Jin, J. Zhou, B. Sun and W. Su, *Synlett*, 2017, **28**, 1321–1326; (*d*) Y. Lv, K. Sun, W. Pu, S. Mao, G. Li, J. Niu, Q. Chen and T. Wang, *RSC Adv.*, 2016, **6**, 93486–93490; (*e*) X. Xu, P. Li, Y. Huang, C. Tong, Y. Yan and Y. Xie, *Tetrahedron Lett.*, 2017, **58**, 1742–1746.

5 (*a*) D. R. G. Brimage, R. S. Davidson and P. R. Steiner, *J. Chem. Soc., Perkin Trans. 1*, 1973, 3563–3572; (*b*) S. Fukuzumi, T. Kitano and T. Tanaka, *Chem. Lett.*, 1989, **18**, 1231–1234.

6 Y. Kurauchi, N. Nobuhara and K. Ohga, *Bull. Chem. Soc. Jpn.*, 1986, **59**, 897–905.

7 A. G. Griesbeck, N. Hoffmann and K.-D. Warzecha, *Acc. Chem. Res.*, 2007, **40**, 128–140.

8 (*a*) J. Libman, *J. Am. Chem. Soc.*, 1975, **97**, 4139–4141; (*b*) K. Tsujimoto, N. Nakao and M. Ohashi, *J. Chem. Soc., Chem. Commun.*, 1992, 366–367; (*c*) H. Yokoi, T. Nakano, W. Fujita, K. Ishiguro and Y. Sawai, *J. Am. Chem. Soc.*, 1998, **120**, 12453–12458.

9 A. John, M. A. Hillmyer and W. B. Tolman, *Organometallics*, 2017, **36**, 506–509.

10 Selected reviews: (*a*) J. M. R. Narayanama and C. R. J. Stephenson, *Chem. Soc. Rev.*, 2011, **40**, 102–113; (*b*)

Open Access Article. Published on 07 October 2020. Downloaded on 8/28/2025 7:18:32 PM. This article is licensed under a Creative Commons Attribution-NonCommercial 3.0 Unported Licence.

C. K. Prier, D. A. Rankic and D. W. C. MacMillan, *Chem. Rev.*, 2013, **113**, 5322–5363; (*c*) N. A. Romero and D. A. Nicewicz, *Chem. Rev.*, 2016, **116**, 10075–10166; (*d*) J. Twilton, C. Le, P. Zhang, M. H. Shaw, R. W. Evans and D. W. C. MacMillan, *Nat. Rev. Chem.*, 2017, **1**, 0052; (*e*) G. E. M. Crisenza and P. Melchiorre, *Nat. Commun.*, 2020, **11**, 803.

11 H. G. Roth, N. A. Romero and D. A. Nicewicz, *Synlett*, 2016, **27**, 714–723.

12 (*a*) A. Juris, V. Balzani, P. Belser and A. von Zelewsky, *Helv. Chim. Acta*, 1981, **64**, 2175–2182; (*b*) K. Kalyanasundaram, *Coord. Chem. Rev.*, 1982, **46**, 159–244.

13 Selected examples: (*a*) L. Chu, C. Ohta, Z. Zuo and D. W. C. MacMillan, *J. Am. Chem. Soc.*, 2014, **136**, 10886–10889; (*b*) A. Noble, S. J. McCarver and D. W. C. MacMillan, *J. Am. Chem. Soc.*, 2015, **137**, 624–627; (*c*) S. Ventre, F. R. Petronijevic and D. W. C. MacMillan, *J. Am. Chem. Soc.*, 2015, **137**, 5654–5657; (*d*) Q.-Q. Zhou, W. Guo, W. Ding, X. Wu, X. Chen, L.-Q. Lu and W.-J. Xiao, *Angew. Chem., Int. Ed.*, 2015, **54**, 11196–11199; (*e*) L. Candish, E. A. Standley, A. G.-S. S. Mukherjee and F. Glorius, *Chem.–Eur. J.*, 2016, **22**, 9971–9974.

14 Decarboxylation reactions of alkyl carboxylic acids using heterogeneous TiO_2-based photocatalysts have been reported: (*a*) D. K. Ellison, P. C. Trulove and R. T. Iwamoto, *Tetrahedron*, 1986, **42**, 6405–6410; (*b*) D. W. Manley, R. T. McBurney, P. Miller, R. F. Howe, S. Rhydderch and J. C. Walton, *J. Am. Chem. Soc.*, 2012, **134**, 13580–13583; (*c*) D. W. Manley and J. C. Walton, *Org. Lett.*, 2014, **16**, 5394–5397.

15 H. Mokbel, D. Anderson, R. Plenderleith, C. Dietlin, F. Morlet-Savary, F. Dumur, D. Gigmes, J.-P. Fouassier and J. Lalevée, *Polym. Chem.*, 2017, **8**, 5580–5592.

16 (*a*) K. Suga, K. Ohkubo and S. Fukuzumi, *J. Phys. Chem. A*, 2006, **110**, 3860–3867; (*b*) H.-T. Song, W. Ding, Q.-Q. Zhou, J. Liu, L.-Q. Lu and W.-J. Xiao, *J. Org. Chem.*, 2016, **81**, 7250–7255; related reactions using cerium salts (*c*) R. A. Sheldon and J. K. Kochi, *J. Am. Chem. Soc.*, 1968, **90**, 6688–6698; (*d*) V. R. Yatham, P. Bellotti and B. König, *Chem. Commun.*, 2019, **55**, 3489–3492; (*e*) S. Shirase, S. Tamaki, K. Shinohara, K. Hirosawa, H. Tsurugi, T. Satoh and K. Mashima, *J. Am. Chem. Soc.*, 2020, **142**, 5668–5675.

17 (*a*) J. D. Griffin, M. A. Zeller and D. A. Nicewicz, *J. Am. Chem. Soc.*, 2015, **137**, 11340–11348; (*b*) L. Candish, L. Pitzer, A. Gómez-Suarez and F. Glorius, *Chem.–Eur. J.*, 2016, **22**, 4753–4756.

18 Selected examples: (*a*) Y. Yoshimi, *J. Photochem. Photobiol., A*, 2017, **342**, 116–130; (*b*) Y. Yoshimi, T. Itou and M. Hatanaka, *Chem. Commun.*, 2007, 5244–5246; (*c*) K. Nishikawa, Y. Yoshimi, K. Maeda, T. Morita, I. Takahashi, T. Itou, S. Inagaki and M. Hatanaka, *J. Org. Chem.*, 2013, **78**, 582–589.

19 The photocatalytic decarboxylative transformation of aromatic carboxylic acids was recently achieved: S. Kubosaki, H. Takeuchi, Y. Iwata, Y. Tanaka, K. Osaka, M. Yamawaki, T. Morita and Y. Yoshimi, *J. Org. Chem.*, 2020, **85**, 5362–5369.

20 For recent reviews of the molecular design of organic photocatalyst, see (*a*) E. Speckmeier, T. G. Fischer and K. Zeitler, *J. Am. Chem. Soc.*, 2018, **140**, 15353–15365; (*b*) J. Mateos, F. Rigodanza, A. Vega-Peñaloza, A. Sartorel, M. Natali, T. Bortolato, G. Pelosi, X. Companyó, M. Bonchio and L. Dell'Amico, *Angew. Chem., Int. Ed.*, 2020, **59**, 1302–1312; (*c*) A. Vega-Peñaloza, J. Mateos, X. Companyó, M. Escudero-Casao and L. Dell'Amico, *Angew. Chem., Int. Ed.*, 2020, DOI: 10.1002/anie.202006416.

21 (*a*) J. Santamaria, R. Ouchabane and J. Rigaudy, *Tetrahedron Lett.*, 1989, **30**, 2927–2928; (*b*) J. Santamaria, M. T. Kaddachi and J. Rigaudy, *Tetrahedron Lett.*, 1990, **31**, 4735–4738.

22 H. Huang, Z. M. Strater, M. Rauch, J. Shee, T. J. Sisto, C. Nuckolls and T. H. Lambert, *Angew. Chem., Int. Ed.*, 2019, **58**, 13318–13322.

23 H. Cheng, X. Wangb, L. Chang, Y. Chen, L. Chu and Z. Zuo, *Sci. Bull.*, 2019, **64**, 1896–1901.

24 C. A. Smith, M. R. Narouz, P. A. Lummis, I. Singh, A. Nazemi, C.-H. Li and C. M. Crudden, *Chem. Rev.*, 2019, **119**, 4986–5056.

25 S. Zhang, J. Zhang, Y. Zhang and Y. Deng, *Chem. Rev.*, 2017, **117**, 6755–6833.

26 M. Villanueva, A. Coronas, J. García and J. Salgado, *Ind. Eng. Chem. Res.*, 2013, **52**, 15718–15727.

27 D. Rottschäfer, B. Neumann, H.-G. Stammler, M. van Gastel, D. M. Andrada and R. S. Ghadwal, *Angew. Chem., Int. Ed.*, 2018, **57**, 4765–4768.

28 H. Baier, A. Kelling, R. Jackstell and H.-J. Holdt, *Z. Anorg. Allg. Chem.*, 2013, **639**, 1731–1739.

29 Electric potential values were determined *vs.* Fc/Fc^+ as a reference and converted to *vs.* SCE using $Fc/Fc^+ = +0.38$ *vs.* SCE: N. G. Connelly and W. E. Geiger, *Chem. Rev.*, 1996, **96**, 877–910. As for the positive potential side of cyclic voltammogram for $BBIm^{2+}\cdot 2[PF_6^-]$, no significant peak was observed. See Fig. S6b in ESI.†

30 $^1E^* = [1/(\lambda_{abs}[nm] \times 8067 \times 10^{-7}) + 1/(\lambda_{em}[nm] \times 8067 \times 10^{-7})] \times 1/2 = 3.58$ eV. $\lambda_{abs} = 290$ nm, $\lambda_{em} = 428$ nm for $BBIm^{2+}$. $^1E^*_{red} = {}^1E^* + E_{red} = +3.58 + (-1.02) = +2.56$ V *vs.* SCE. $^3E^*_{red} = {}^3E^* + E_{red} = +1.91 + (-1.02) = +0.89$ V *vs.* SCE, where $^3E^*$ was determined from the phosphorescence spectrum ($\lambda_{max} = 641$ nm) observed in an ethanol glass at 77 K.

31 (*a*) P. B. Merkel, P. Luo, J. P. Dinnocenzo and S. Farid, *J. Org. Chem.*, 2009, **74**, 5163–5173; (*b*) K. Ohkubo, T. Kobayashi and S. Fukuzumi, *Opt. Express*, 2012, **20**, A360–A365; (*c*) S. Fukuzumi, K. Ohkubo, T. Suenobu, K. Kato, M. Fujitsuka and O. Ito, *J. Am. Chem. Soc.*, 2001, **123**, 8459–8467.

32 S. Fukuzumi, H. Kotani, K. Ohkubo, S. Ogo, N. V. Tkachenko and H. Lemmetyinen, *J. Am. Chem. Soc.*, 2004, **126**, 1600–1601.

33 The quantum yields for the decarboxylative hydroxylation reaction of **4a** with photocatalysts $BBIm^{2+}\cdot 2[PF_6^-]$, $\mathbf{1}^+\cdot[Br^-]$ and $Acr\text{-}Mes^+\cdot[ClO_4^-]$ were determined using a 365 LED lamp (60 W) as the light source under the same absorbance condition [abs. at 365 nm = 1.0]. The quantum yield for the photocatalytic oxygenation of *p*-xylene with

 This journal is © The Royal Society of Chemistry 2020

Open Access Article. Published on 07 October 2020. Downloaded on 8/28/2025 7:18:32 PM.
This article is licensed under a Creative Commons Attribution-NonCommercial 3.0 Unported Licence.

Acr-Mes$^{+}\cdot[ClO_4{}^{-}]$ was used as a reference value: K. Ohkubo, K. Mizushima, R. Iwata, K. Souma, N. Suzuki and S. Fukuzumi, *Chem. Commun.*, 2010, **46**, 601–603. Yield/irradiation time profiles are shown in Fig. S4 and the quantum yields were summarized in Table S2 in ESI.†

34 (*a*) H. Kolbe, *Ann. Chem. Pharm.*, 1848, **64**, 339–341; (*b*) F. Minisci, E. Vismara, G. Morini, F. Fontana, S. Levi and M. Serravalle, *J. Org. Chem.*, 1986, **51**, 476–479; (*c*) M. H. Habibi and S. Farhadi, *Tetrahedron Lett.*, 1999, **40**, 2821–2824.

35 A. Albini and S. Spreti, *J. Chem. Soc., Perkin Trans. 2*, 1987, 1175–1179.

36 H. Boaz and G. K. Rollefson, *J. Am. Chem. Soc.*, 1950, **72**, 3435–3443.

37 Notes: (*a*) The intensity of the fluorescence of $BBIm^{2+}$ apparently increased with increasing amount of added sodium pivalate, which is likely due to a significant structural change by complexation between $BBIm^{2+}$ and pivalate. We were able to isolate $BBIm^{2+}\cdot[t\text{BuCOO}^{-}][PF_6{}^{-}]$, which was immediately formed by mixing $BBIm^{2+}\cdot 2[PF_6{}^{-}]$ and sodium pivalate in CH_3CN; (*b*) The yield of photocatalytic decarboxylative dimerisation was not significantly affected by the concentration of $BBIm^{2+}$, suggesting that the short-lived $^{1}BBIm^{2+*}$ is not an active species for the reaction; (*c*) In addition to the short life time, another possible reason for the absence of fluorescence quenching by $t\text{BuCOO}^{-}$ in spite of the highly negative driving force is that the process is located in the Marcus inverted region: R. A. Marcus, *Annu. Rev. Phys. Chem.*, 1964, **15**, 155–196.

38 T. N. Das, T. Dhanasekaran, Z. B. Alfassi and P. Neta, *J. Phys. Chem. A*, 1998, **102**, 280–284.

39 ^{18}O labeling experiments were performed to confirm the origin of oxygen atom in **5a**. When the photocatalytic hydroxylation reaction was conducted in $^{18}O_2$-saturated acetonitrile using **4a** as a substrate, [^{18}O]**5a** was detected by HRMS (Fig. S3a in ESI†). Similarly, when the reaction was performed in non-labeled O_2-saturated acetonitrile, only [^{16}O]**5a** was detected and no [^{18}O]**5a** was observed (Fig. S3b in ESI†). This result indicates that the oxygen in the **5a** product is derived from O_2.

40 The use of water decreased the oxygen concentration in the system, which increased the yield of the dimerisation product. Indeed, when the reaction was conducted in acetonitrile using **6a** as a substrate, the yield of the dimer decreased to 24% and hydroxylation proceeded in 41% yield. There is a difference in the solubility of oxygen between water (1.3 mM) and acetonitrile (13 mM), see (*a*) I. Nakanishi, S. Fukuzumi, T. Konishi, K. Ohkubo, M. Fujitsuka, O. Ito and N. Miyata, *J. Phys. Chem. B*, 2002, **106**, 2372–2380; (*b*) S. Fukuzumi, S. Fujita, T. Suenobu, H. Yamada, H. Imahori, Y. Araki and O. Ito, *J. Phys. Chem. A*, 2002, **106**, 1241–1247; (*c*) S. Fukuzumi, M. Ishikawa and T. Tanaka, *J. Chem. Soc., Perkin Trans. 2*, 1989, 1037–1045.

41 D. T. Sawyer, T. S. Calderwood, K. Yamaguchi and C. T. Angelis, *Inorg. Chem.*, 1982, **22**, 2577–2583.